Surface morphology-optical properties relationship in thermochromic VO thin films obtained by air oxidation of vanadium nitride

A C García-Wong, D Pilloud, S Bruyère, D Mangin, S Migot, J F Pierson, F Capon

Journal of Materiomics 7 (2021) 657–664

Contents lists available at ScienceDirect

Journal of Materiomics

journal homepage: www.journals.elsevier.com/journal-of-materiomics/

Opinion paper

Surface morphology-optical properties relationship in thermochromic VO_2 thin films obtained by air oxidation of vanadium nitride

A.C. García-Wong, D. Pilloud, S. Bruyère, D. Mangin, S. Migot, J.F. Pierson*, F. Capon

Institut Jean Lamour (UMR CNRS 7198), Université de Lorraine, 54000, Nancy, France

ARTICLE INFO

Article history:
Received 24 August 2020
Received in revised form
23 November 2020
Accepted 10 December 2020
Available online 15 December 2020

Keywords:
Vanadium dioxide
Vanadium nitride
Thermochromism
Optical properties
Air oxidation

ABSTRACT

In this paper, vanadium nitride (VN) thin films have been deposited on Al substrates by reactive magnetron sputtering. Thermochromic VO_2 films have been obtained by air oxidation of VN samples performed at three temperatures (450, 525 and 550 °C) at various durations (lower than 50 min). X-ray diffraction and Raman spectrometry of the VN oxidized films indicate that VO_2 and V_2O_5 are the only phases produced during the oxidation process. Vanadium dioxide is the first oxide formed. It coexists with VN in a long period at 450 °C or suddenly disappears at 525 and 550 °C. Whatever the temperature, V_2O_5 is exclusively detected after the total oxidation of VN. This oxide is detrimental to the thermochromic performance of films. The emissivity-switching properties of the oxidized films were analyzed by infrared camera in the 7.5–13 μm range. The comparison among all the samples exhibiting a thermochromic behavior shows that the maximum emissivity switch is independent of the oxidation temperature and the surface morphology of the samples. These results could open a new strategy in the investigation of VN oxidation as a method to obtain VO_2, along with an insight into the correlation between surface morphology and optical properties.

1. Introduction

Vanadium dioxide (VO_2) has been one of the most studied thermochromic materials since its discovery by Morin in 1959 [1]. It undergoes a reversible metal-insulator transition (MIT) from a monoclinic to a tetragonal rutile phase approximately at $T_{MIT} = 68$ °C. Below the transition temperature, VO_2 exhibits high transmittance in the infrared region and high electrical resistivity, whereas above T_{MIT} it presents low transmittance and low electrical resistivity [2]. The significant change in optical transmittance and reflectance, particularly in the infrared (IR) region makes this material suitable for numerous applications, for instance as smart windows [3–8], smart radiator devices for spacecraft [9–13], thermal solar collectors [14–16], IR bolometers detectors [17,18], infrared camouflage [19–22]…

However, to employ VO_2 as smart coating some challenges need to be overcome. For example, in the case of smart windows: the luminous transmittance (T_{lum}) and solar transmittance modulation (ΔT_{sol}) have to be high. On the other hand, the transition temperature of the material should be close to room temperature, therefore T_{MIT} of the VO_2 should be lowered [23]. There are different strategies to improve the thermochromic performance of VO_2 thin films. The selection of the substrate can influence the switching performance of the material [24,25]. Nevertheless, the substrate choice is linked directly to the desired application. Elemental doping is one of the most practical and feasible methods to tune the optical properties of VO_2 films as well as change T_{MIT}. It has been shown that W is one of the most successful elements to reduce T_{MIT} of VO_2 films [26,27]. On the contrary, Krammer et al. proved that T_{MIT} could be increased to approx. 94 °C by Ge doping [28]. Several dopants (Mg, Ca, Sr, Ba, Al, Sn, among others) have been studied as an effective way to enhance the optical properties of VO_2 films [15,23,29–32]. Moreover, it has been proven that some anti-reflective coatings can improve the optical properties of VO_2 films (ZrO_2 [33], TiO_2 [34,35]). Furthermore, anti-reflective layers such as TiO_2 [6,34], SiO_2 [36], AZO [37] and SiN_x [38] have been used to prevent further oxidation (in case the films continue to be in air-direct contact).

Although great advances have been made in the thermochromic properties of VO_2, the synthesis of this material on large surfaces is still an issue. Since the vanadium-oxygen binary system contains plenty of oxides with a stoichiometry close to that of VO_2 [39],

* Corresponding author.
E-mail address: jean-francois.pierson@univ-lorraine.fr (J.F. Pierson).
Peer review under responsibility of The Chinese Ceramic Society.

https://doi.org/10.1016/j.jmat.2020.12.005

perfect control of the oxygen content is required on the whole surface of the substrate. Using the conventional magnetron sputtering process, such composition control is hardly achieved. An alternative method to grow VO_2 on large surfaces is to use a two-step process: deposition of a metallic vanadium film followed by an air-controlled oxidation step to synthesize the pure VO_2 phase [40]. In a recent paper, we proposed a new strategy to obtain high-quality VO_2 films by the controlled oxidation of vanadium nitride films (VN) deposited on Si substrate [41]. The latter allowed us to generate a phase diagram of VN thin film oxidation at 450 °C.

In the present work, VN thin films were reactively sputter-deposited on Al substrates. The air oxidation of VN samples is performed at three temperatures (450, 525 and 550 °C) and several durations up to 50 min. We study the effect of the temperature and the oxidation duration on the formation of VO_2 films. We aim to determine the influence of the oxidation parameters on the functional properties of the obtained VO_2 films.

2. Experimental details

An in-line semi-industrial sputtering machine was used to deposit the VN thin films. The volume of the chamber is approx. 350 L. The substrate holder offers the possibility to produce samples with a 29 × 19 cm^2 surface. Aluminum (Al) foils of this size were used as substrates. Several silicon pieces (2 × 2) cm^2 were also placed on the Al substrate. This method provides samples with the same thickness on different substrates in a single run. To guarantee films homogeneity the substrate holder moved back and forth in front of the V target at a speed of 50 cm/min during 1 h (Fig. 1 a shows a well-simplified scheme of the semi-industrial chamber). The VN films were deposited using a metallic vanadium target (33 cm length, 5 cm width, 0.6 cm thick and 99.95% purity) in an Ar–N_2 reactive mixture. The flow rates of argon and nitrogen were fixed to 30 and 5 standard cubic centimeters per minute (sccm), respectively. The V target was powered by a pulsed-DC power supply (Pinnacle + Advanced Energy) with a current fixed at 1.5 A. The frequency of DC-pulses and their off-time were kept at 50 kHz and 4 μs, respectively. The total pressure measured with an MKS Baratron gauge was fixed to 1 Pa. The VN films were deposited without external heating and the target to substrate distance was 5 cm. The thickness of the films (175 nm) was measured by a Bruker DektakXT tactile profilometer.

To obtain thermochromic VO_2, the VN films were annealed in a Carbolite HRF 7/45 furnace adapted with a sample tray loader to avoid the drop of temperature when inserting the samples. The air annealing was performed at three different temperatures (450, 525 and 550 °C) and various durations (from a few min up to 50 min). The films were labeled "VN" for as-deposited vanadium nitride films and "VNtemperature_time" for the oxidized films at various temperatures and annealing duration.

X-ray diffraction (XRD) measurements were conducted in a θ-2θ configuration with Cu $K_{\alpha 1}$ radiation (λ = 1.5406 Å) using a Bruker D8 Advanced diffractometer. The Raman spectra were measured with a Horiba Jobin-Yvon LabRAM spectrometer. A Nd:YAG laser (532 nm wavelength) was used as the excitation source. To avoid local heating effects (such as oxidation from VO_2 to V_2O_5), the power of the laser beam was controlled to approx. 10 mW. The microstructural characterization of the sample surfaces was

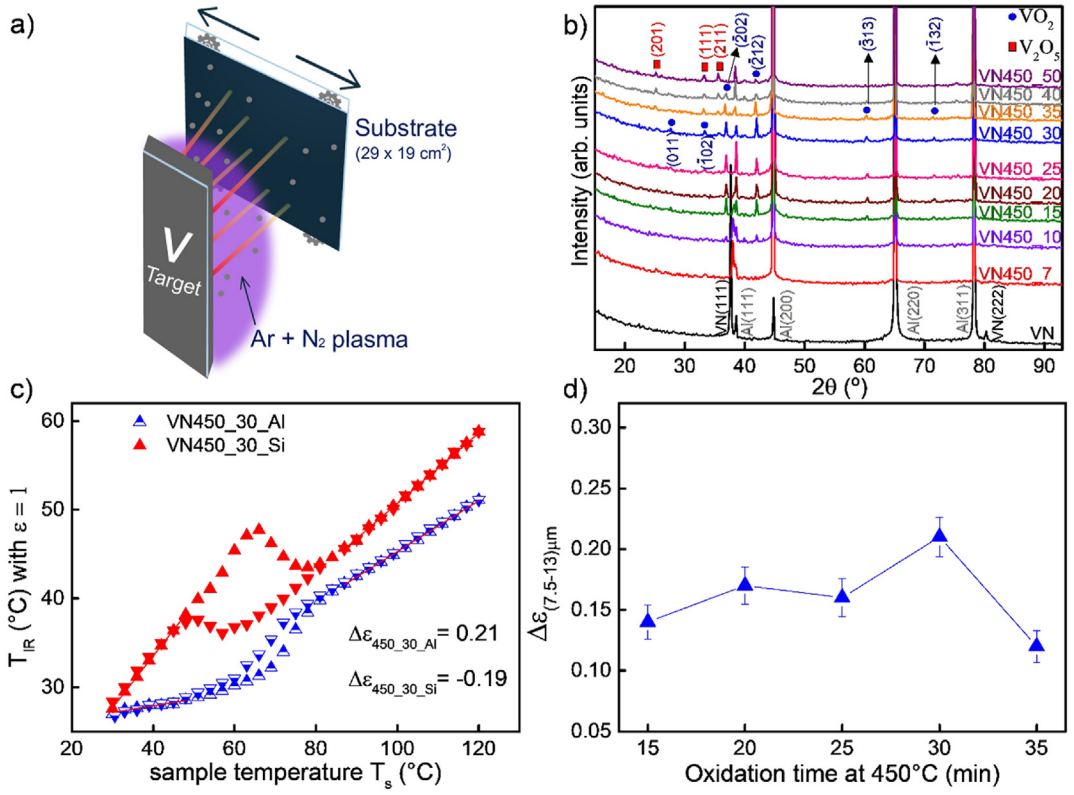

Fig. 1. a) Scheme of the semi-industrial sputtering machine used to deposit VN precursors films. Different from lab-scale sputtering chambers, the substrate holder moved back and forth in front of the V target to ensure films homogeneity. b) X-ray diffractograms of as-deposited VN film on aluminum substrate and the resulting oxidized films after air annealing at 450 °C for various durations. c) Thermal camera measurements of apparent infrared temperatures (T_{IR}), as a function of sample temperature (T_s) for VN films on Al and Si substrates oxidized during 30 min. Up and down triangles represent the profiles for temperature ramping up and down, respectively. The red lines obtained by a linear fitting in the low-temperature (LT) and high-temperature region (HT) enabled the determination of emissivity values before and after MIT. d) Dependence of the emissivity switch (on the range of 7.5–13 μm) with the oxidation time at 450 °C for samples on Al substrates showing a thermochromic behavior.

observed by scanning electron microscopy (SEM) in a Philips FEG XL 30. Transmission electron microscopy (TEM) was performed in the VN525_3 sample with a JEOL ARM 200-Cold FEG (point resolution 0.19 nm). For this analysis, a cross-section TEM sample of the film was prepared by a focused ion beam FIB-SEM dual beam system (FEI Helios Nanolab 600i). An IMS 7F Cameca secondary ions mass spectrometry system was used to obtain the compositional profiles of the films as a function of depth. The instrument was configured to have Cs^+ primary ion energy of 5 keV, secondary ion energy of 2 keV, a raster size of 100 μm and an analyzed area of 63 μm.

The study of optical properties of the films as a function of the temperature (30–120 °C range) was performed using a FLIR A300 infrared camera (IR) with a spectral IR wavelength from 7.5 to 13 μm. The camera is supported by the ResearchIR software package. The emissivity of the oxidized films was calculated from the slope of the temperature measured using the IR camera (T_{IR}) as a function of the real temperature (T_s) of the sample. Measurements were accomplished by considering $\varepsilon = 1$ regardless of the sample. A Präzitherm heater system controlled and measured the T_s of each sample. The emissivity switch, $\Delta\varepsilon = \varepsilon_{HT} - \varepsilon_{LT}$ was calculated by the difference between the slopes corresponding to each region of the MIT according to the method employed by Benkahoul et al. [13]. ε_{HT} and ε_{LT} correspond to the emissivity at high and low temperatures, respectively.

3. Results

3.1. Thermochromic behavior of oxidized VN samples at 450 °C

VN precursor thin films (175 nm thick) have been deposited by the sputtering of a vanadium target in a reactive Ar–N_2 atmosphere on Al substrate (Fig. 1 a)). The films have been air oxidized at 450 °C during different durations. As-deposited VN films exhibit two peaks corresponding to (111) and (222) planes of the face-centered cubic VN structure (PDF no.00-035-0768), located at approx. 37.9° and 80.3°, respectively (Fig. 1 b)). No other peaks are detected except those coming from the aluminum substrate. The X-ray results for films annealed at 450 °C during various durations in the 7–50 min range are also presented in Fig. 1 b). After 7 min of annealing, the VO_2 phase is not detected. Nevertheless, the oxidation process started, as evidenced by the decline of the VN peak intensity. Besides, these peaks are shifted to higher angles due to stress relaxation during the oxidation process. VN peaks intensity continues to decrease as the annealing time increases, and the main (111) peak disappears at 25 min, indicating that the sample is completely oxidized. On the other hand, after 10 min of air oxidation, a first peak corresponding to the $(\bar{2}12)$ monoclinic (m)–VO_2 is detected for the first time close to 42.0°. As oxidation continues, other peaks located at approx. $2\theta = 27.8$, 33.3, 36.7, 60.3 and 71.4° (PDF no. 04-003-2035) emerge belonging to m-VO_2. The intensities of these different peaks indicate that the oxide layer does not grow with a strong preferred orientation. Since the as-deposited VN films exhibit a texture along the [111] direction and because the m-VO_2 grains present several diffraction peaks, it may be concluded that there is no structural relationship between the VN and the m-VO_2 grains. Results between 10 and 25 min suggest that within this period m-VO_2 is formed from the VN precursor oxidation. The most intense peak of VO_2 appears at 30 min of oxidation when there is no VN peak anymore (see Fig. S1 supplementary information). All samples oxidized more than 35 min show three peaks that correspond to the orthorhombic V_2O_5 phase (PDF no. 00-041-1426). Once again there is a competition between phases, in this case, the over-oxidation of VO_2 leads to the formation of the most stable phase of the V–O system i.e., V_2O_5. For the VN450_50 sample, the VO_2 diffraction peaks almost disappeared, and V_2O_5 becomes the predominant crystalline phase. These results are in agreement with our previous work on silicon substrate [41] and also with several authors who already proved the transition from V^{4+} state to V^{5+} state as the oxidation time increases [42,43].

Among the exciting change in properties during the phase transition on VO_2, the emissivity switch provides an excellent idea of the thermochromic response of the films. The higher the difference in emissivity between the monoclinic and the tetragonal phase of VO_2, the better the thermochromic properties. Fig. 1 c) shows the apparent infrared temperature as a function of the real temperature of two samples oxidized during 30 min at 450 °C on different substrates (Al and Si). Both samples present a good thermochromic performance. There are two important features to discuss in this figure: first the difference in sign in the emissivity switch. Benkahoul et al. disclosed that VO_2 deposited on highly IR-reflective substrates such as Al exhibit opposite behavior to VO_2 deposited on IR-transparent substrates such as Si and quartz [13]. Hence, the choice of the substrate is directly related to the desired application (applications in the solar thermal domain required a highly IR-reflectivity substrate). Second, the significant difference in the hysteresis width of both systems is related to the distinct VO_2 film grow orientation in each substrate (compare Fig. 1 in Ref. [41] and Fig. 1 b)) [44].

Fig. 1 d) displays the dependence of the emissivity switch in the 7.5–13 μm range as a function of the annealing duration at 450 °C for films deposited on aluminum substrates. The values of $\Delta\varepsilon$ are ranging from 0.12 to 0.21 (see Fig. S2 in the supplementary information). A tendency to increase the $\Delta\varepsilon$ until a maximum value at 30 min of oxidation is the result of the competing effect of VN oxidation and the growth of VO_2. However, with higher oxidation duration the formation of V_2O_5 starts and affects the thermochromic effect. Following the same line of thought due to the increasing (decreasing) presence of V_2O_5 (VO_2) samples with 40 and 50 min of oxidation do not exhibit thermochromic response anymore. Moreover, samples oxidized less than 15 min with an important residual VN layer (see Fig. S1 in the supplementary information) present a poor thermochromic performance. These findings are in agreement with XRD and also with our previous results [41]. The difference between the present work and our previous one corresponds to the nature of the substrate: Al vs. Si. The type of substrate does not modify the structure of the films. Thermochromic behavior is obtained for both substrates for very close annealing durations. The main difference is related to the sign of the emissivity switch that is positive using a reflective substrate (Al) and negative using an IR-transparent substrate (Si).

3.2. Thermochromism performance on oxidized VN samples at 525 °C and 550 °C

To study the effect of air oxidation at higher temperatures on the thermochromic behavior, VN precursor thin films were annealed at 525 °C and 550 °C during distinct durations. Compared to section 3.1, the annealing temperature has been increased, as a consequence, the annealing duration has been reduced to take into account the increase of the oxidation kinetics. Fig. 2 a) (Fig. 2 b)) depicts the diffractograms for samples oxidized at 525 °C (550 °C) between 3 and 7 min (2–5 min). The corresponding XRD results for VN film (equal to those displayed in Fig. 1 b)) are included as a guideline for a better comparison of the oxidation process. Sample VN525_3 displays several peaks corresponding to m-VO_2 and the signal of VN almost disappeared, indicating that the oxidation is almost complete. VO_2 is the only oxide presents on the samples oxidized between 3 and 5 min, besides VN peaks completely

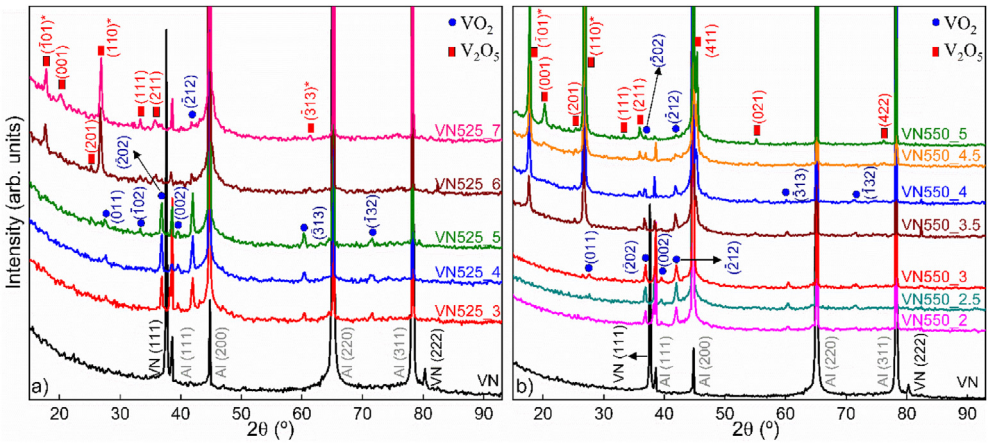

Fig. 2. X-rays diffractograms of as-deposited VN film on aluminum substrate and the resulting oxide films after air oxidation at a) 525 °C and b) 550 °C for various durations.

vanished at 5 min. The maximum intensity of VO_2 peaks are detected after 5 min, following the oxidation process, these peaks rapidly decrease in intensity and almost fade away after 7 min. In contrast, after 5 min of oxidation, intense peaks of V_2O_5 emerge caused by the over-oxidation of m-VO_2. Interestingly, a monoclinic V_2O_5 phase (PDF no. 00-061-0027) is revealed together with the already detected orthorhombic V_2O_5 phase (PDF no. 00-041-1426). The peaks of the m-V_2O_5 are situated around $2\theta = 17.8$, 26.8 and 61.4° and identified with an asterisk (*) in the figure.

The X-ray diffractograms of samples oxidized at 550 °C, Fig. 2 b) are similar to those reported at 525 °C (Fig. 2 a)). The only phase of the V–O system detected among 2 and 3 min is m-VO_2. For higher durations, peaks corresponding to monoclinic and orthorhombic V_2O_5 phase arise due to the over-oxidation of VO_2. During this period the intensity of the peaks belonging to m-VO_2 starts to decrease inducing a vanishing of this phase after 5 min of oxidation.

The X-ray results for the three studied temperatures suggest that the VN oxidation occurs on the same stages. The first phase of the V–O system detected is m-VO_2 that could coexist with VN. The second and third phases are orthorhombic and monoclinic V_2O_5, which always appeared only when there is no signal of VN anymore. Yet again, these results illustrate the change from the V^{4+} state into the V^{5+} state with the oxidation time increase and are consistent with the findings of previous studies [41–43].

Oxidation kinetics seems to be the main difference in the annealing process between 525 °C and 550 °C, according to X-ray results. The phases belonging to the binary V–O system crystallize in structures with low symmetries giving a high amount of diffraction peaks. The application of the sole XRD method to characterize the oxide layer may induce some mistakes in the film structure determination. Thus, the use of a second characterization method is mandatory. Within this objective, we have employed Raman spectrometry. Fig. 3 presents room-temperature Raman spectra of oxidized VN films between 3 and 5 min at 525 °C and 550 °C.

The samples annealed at 525 °C and the VN550_3 one show similar vibration bands (located at approx. 194, 224, 263, 389 and 624 cm^{-1}) that can be assigned to m-VO_2 phase, in agreement with the literature [45–48]. In the case of the oxidized films at 550 °C during 4 and 5 min, the shape of the spectra is different from the other samples. Some vibration bands still correspond to VO_2, yet new bands are detected at approx. 195, 282, 301, 405 and 532 cm^{-1} that are readily ascribed to the orthorhombic V_2O_5 phase [45,49]. These findings confirm the simultaneous presence of VO_2 and V_2O_5 in VN550_4 and VN550_5 samples as well as the only existence of

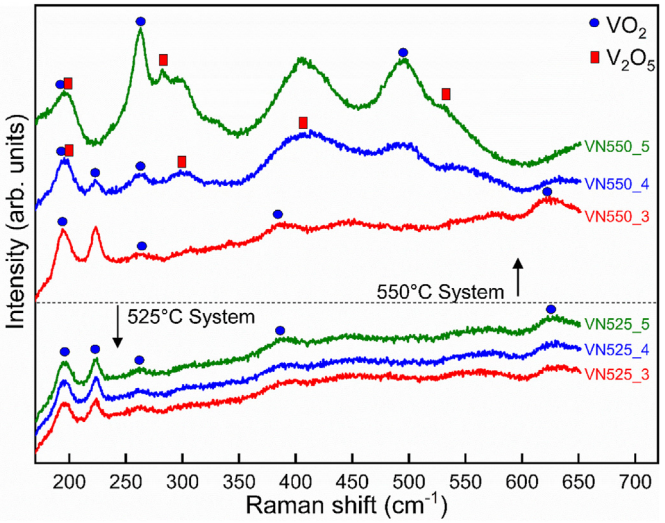

Fig. 3. Raman spectra of air-oxidized VN films during 3–5 min at 525 °C and 550 °C.

m-VO_2 in samples oxidized between 3 and 5 min at 525 °C and 3 min at 550 °C as shown by the X-ray results.

SIMS is a well-known surface analysis technique suitable to obtain composition depth profiles. The SIMS capability of depth profiling with high resolution turns out useful to check the presence of a possible residual layer of VN between the substrate and the formed VO_2 layer. Fig. 4 a), c) and d) show the SIMS depth profile of samples oxidized at 525 °C for 3, 4 and 5 min respectively. Starting from the sample surface the signal intensities for V, N, O and Al elements are displayed as a function of etching time in each of the three samples. The twenty first seconds of the analyses (until V and O lines cross each other) can be omitted, it corresponds to the depth needed to reach an equilibrium state. The signal corresponding to V and O in Fig. 4 a) is relatively constant during the first 400 s, suggesting the presence of vanadium oxide with a constant composition. During this period the amount of N is negligible thanks to VN oxidation. On the contrary, after 400 s the intensity of these three elements changes, the signal of O drops while the opposite occurs for V and N. The latter evince the presence of a remaining VN layer in the VN525_3 sample. Fig. 4 b) shows a transmission electron microscopy cross-section of the VN525_3 sample. The figure depicts close to the Al substrate an uninterrupted columnar VN layer of approx. 90 nm thick and above a VO_2

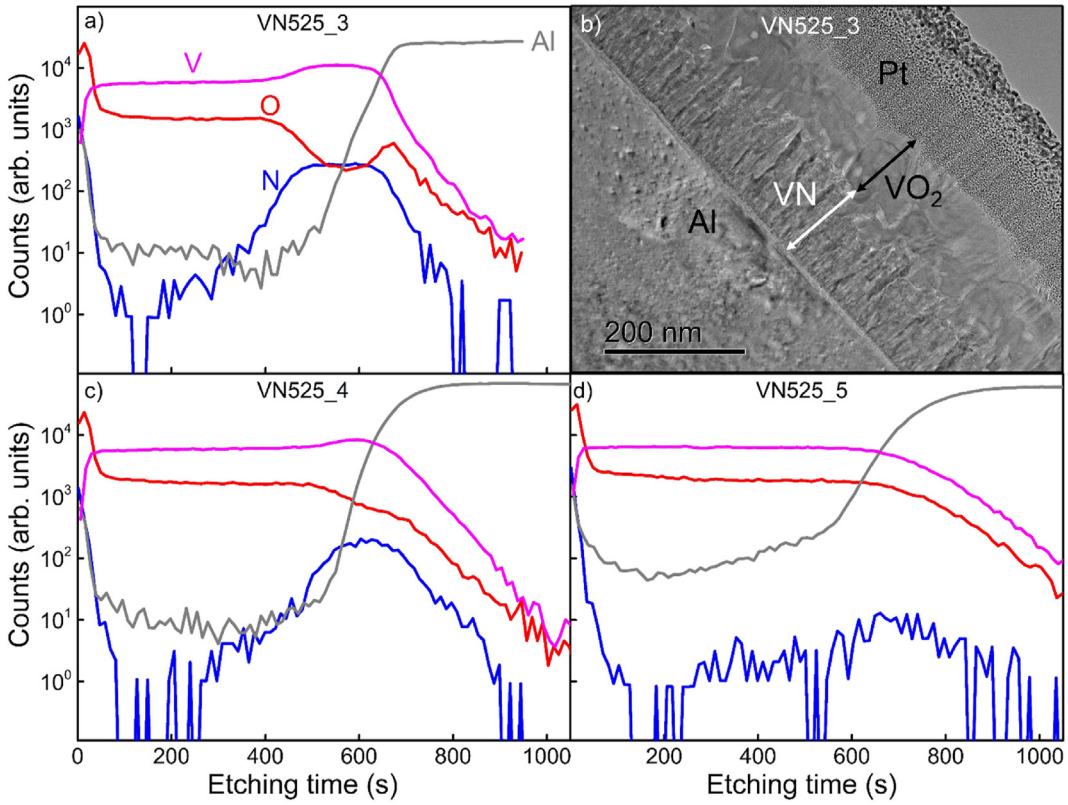

Fig. 4. SIMS depth profiles of samples oxidized at 525 °C during 3, 4 and 5 min for a), c) and d), respectively. The etching time indicates the depth of the sample from the surface. b) TEM cross-section image of sample VN525_3.

layer of approx. 140 nm thick (corresponding to the oxidation of an 85 nm thick VN layer). This TEM cross-section image confirms the results obtained by SIMS. From Fig. 4 a) and b) it can be concluded that the sample VN525_3 is not completely oxidized. The behavior of V, N and O signals from Fig. 4 c) is equivalent to Fig. 4 a), however, the thickness of the remaining VN layer is lower compared to the sample VN525_3. Moreover, V and O signals are rather constant throughout all the depth profile of sample VN525_5 (Fig. 4 d)) and N amount is negligible, suggesting that the sample is fully oxidized. The SIMS analysis corroborates the X-ray results of Fig. 2 a) showing the growing presence of VO_2 caused by the air oxidation of VN.

Fig. 5 depicts the top view SEM images of six noteworthy samples: the as-deposited VN films and samples oxidized during 15, 30 min at 450 °C, 4, 5 min at 525 °C and 3 min at 550 °C. Note that all the images have not the same magnification, but all of them except the as-deposited VN were acquired with identical acceleration voltage. The as-deposited VN film exhibits a surface morphology with small tetrahedral grains in agreement with the [111] preferred orientation evidenced by XRD (as the VN films on Si substrate [41]). Along the oxidation process, the morphology of the oxidized samples considerably changes when compared to the VN films (Fig. 5 a)). After 15 min of oxidation at 450 °C (Fig. 5 b)), the oxidized VN grains merge into an extended structure, enlarging grain size. Increasing the annealing time at the same temperature leads to the growth of the grains (Fig. 5 c)). Samples VN525_4 (Fig. 5 d)) and VN525_5 (Fig. 5 e)) present different morphology than samples oxidized at 450 °C, the grains are bigger and more rounded. In the case of Fig. 5 f) (VN550_3) the grains are equiaxed and are the largest among all the images. It is noteworthy that despite drastic different morphology and grain size the images of Fig. 5 c), e) and f) correspond to samples completely oxidized, in which the only phase detected is m-VO_2.

The optical modulation properties in the 7.5–13 μm IR domain for samples oxidized at 525 °C in a range of 3–6 min are studied with an infrared camera (Fig. 6 a)). Air-annealed samples between 3 and 5 min display hysteresis loops near the MIT region, a characteristic thermochromic signal. The corresponding values for the emissivity switch for these samples slightly increase with oxidation time. This is a consequence of the continuous growth of VO_2 from the oxidation of VN, reaching a maximum after 5 min. However, the $\Delta\varepsilon$ value of VN525_6 drops drastically to 0.05 (75% less when compared with the VN525_5 sample) caused by the over-oxidation of VO_2 to V_2O_5. This behavior is in total accordance with X-ray and Raman results (Fig. 2 a) and Fig. 3).

Fig. 6 b) displays the dependence of the emissivity switch with oxidation time for the three studied systems (see Supplementary Information Fig. S3 for the 550 °C system). All systems have similar dynamics. The $\Delta\varepsilon$ values increase smoothly when VN and VO_2 phase coexist, until reaching a maximum value when VO_2 is the predominant phase and the precursor is completely oxidized. Further increase of the oxidation time induces a decrease of $\Delta\varepsilon$ due to the over-oxidation of VO_2 and the consequent growth of V_2O_5. The optical modulation properties' findings are in full agreement with XRD and Raman results.

Several stimulating conclusions can be drawn from Fig. 6 b). First of all, the maximum values of $\Delta\varepsilon$ are similar (between 0.20 and 0.22) for the three different systems suggesting that they are independent of the oxidation temperature. These results could be related to the fact that all the precursor VN samples have the same thickness. The amount of VN which can be transformed into VO_2 is the same, independent of the air-annealed temperature. The emissivity contrast values found in this paper are in the same range

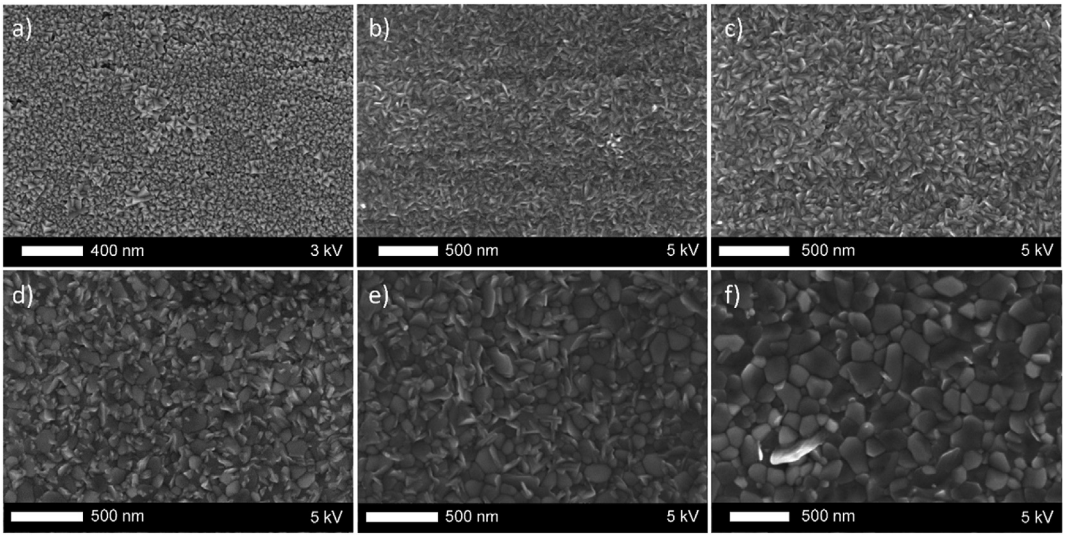

Fig. 5. Top-view SEM images corresponding to a) the as-deposited VN films and samples VN450_15, VN450_30, VN525_4, VN525_5 and VN550_3 for b), c), d), e) and f), respectively. Note that the magnification is different, as indicated in each image, besides the image of the as-deposited VN was acquired with a lower acceleration voltage.

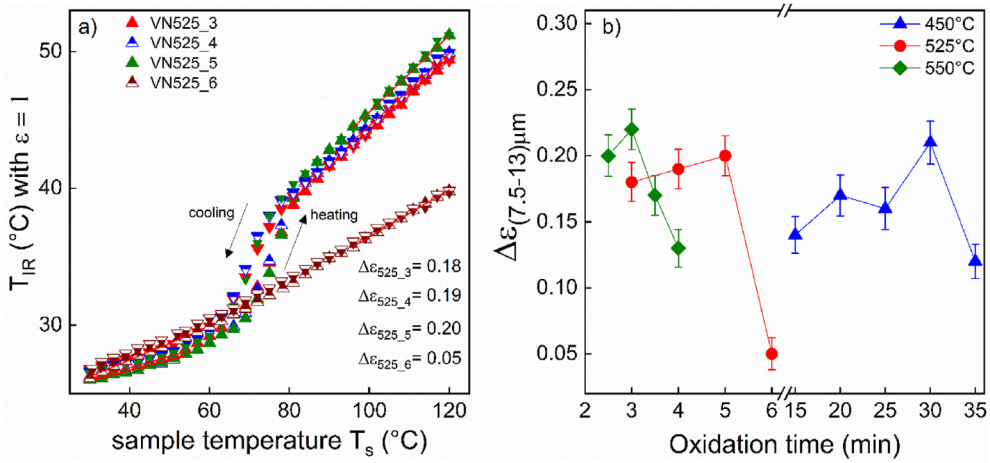

Fig. 6. a) Thermal camera measurements of apparent infrared temperatures (T_{IR}), as a function of sample temperature (T_s) for VN films oxidized at 525 °C between 3 and 6 min. Measurements are carried out by considering $\varepsilon = 1$ irrespective to the sample. Up and down triangles represent the profiles for temperature ramping up and down, respectively. The red lines obtained by a linear fitting in the low temperature (LT) and high temperature region (HT) enabled the determination of emissivity values before and after MIT. b) Dependence of the emissivity switch (on the range of 7.5–13 μm) with the oxidation time for the three studied systems (450, 525 and 550 °C).

as those reported in the literature in the same IR domain. For instance, Benkahoul et al. found $\Delta\varepsilon = 0.26$ in 300 nm thick VO_2 film deposited on Al using an infrared camera in the 8–14 μm range [13].

It is well reported in the literature the close correlation between electrical properties with the surface morphology of VO_2 [50–52]. However, the morphology of the samples with the highest emissivity switch (VN450_30, VN525_5 and VN550_3) in the different studied systems is remarkably different (Fig. 5 c), e) and f) respectively). These results suggest that the optical properties are independent of the VO_2 surface morphology, at least in the 7.5–13 μm IR range.

One more interesting result is related to the best-oxidation time for each studied temperature. Xu et al. [53] reported an optimal oxidation time at different temperatures to obtain high-quality VO_2 films by oxidation of 100 nm thick vanadium films (using the Sputtering Oxidation Coupling method [40]). Besides, they managed to calculate the diffusion activation energy of the oxidation process. A direct evaluation of the results of both works shows that the values of activation energy are similar (see Fig. S4 in supplementary information). Yet, the more important result from the comparison is that the time required to obtain the best VO_2 is larger in VN than in V films, indicating that it is easier to control the oxidation of VN films.

4. Conclusions

This work is dedicated to the synthesis of thermochromic VO_2 thin films from the air oxidation of VN thin films. We study the effect of three temperatures oxidation (450, 525 and 550 °C) on the optical properties in the 7.5–13 μm range. Throughout the oxidation process at the three temperatures, VO_2 and V_2O_5 are the only phases detected. During the oxidation process, the first oxide formed is VO_2, it coexists with VN in a long period at 450 °C or suddenly disappeared at 525 and 550 °C. Furthermore, V_2O_5 is detected after the total oxidation of VN. These findings confirm the

oxidation from the V^{4+} state into the V^{5+} state with the annealing time increase and correspond with the results of previous studies.

Concerning the optical properties of the oxidized films, the best emissivity switch in each system is quite similar (between 0.20 and 0.22) independently of the oxidation temperature. On the other hand, the film morphology is strongly dependent on the oxidation temperature. Nevertheless, the change of the surface morphology does not influence the optical properties of the films. This indicates that the optical properties of VO_2 in the 7.5–13 μm range are independent of the surface morphology.

Due to the simplicity of producing VN thin film on large surfaces and different substrates, as well as the good optical modulation properties of oxidized films at different temperatures and durations, the VN oxidation process seems encouraging for the production of high-quality thermochromic VO_2 films for furtivity and smart radiator devices.

Declaration of competing interest

The authors declare that they have no known competing financial interests or personal relationships that could have appeared to influence the work reported in this paper.

Acknowledgments

This work was supported by the French PIA project “Lorraine Université d’Excellence”, reference ANR-15-IDEX-04-LUE. The authors acknowledge the financial support of the Contrat de Plan Etat-Région MatDS. They are also grateful to the *Centre de Compétences* Dᴀvm (cc-Dᴀvm) of the Institut Jean Lamour for the semi-industrial chamber provision, to the *Centre de Compétences* X-gamma for the access to X-ray diffraction system and to Mrs P. Miranda d’Assunção for the design of semi-industrial sputtering chamber scheme.

Appendix A. Supplementary data

Supplementary data to this article can be found online at https://doi.org/10.1016/j.jmat.2020.12.005.

References

[1] Morin FJ. Oxides which show a metal-to-insulator transition at the neel temperature. Phys Rev Lett 1959;3:34–6. https://doi.org/10.1103/PhysRevLett.3.34.
[2] Barker AS, Verleur HW, Guggenheim HJ. Infrared optical properties of vanadium dioxide above and below the transition temperature. Phys Rev Lett 1966;17:1286–9. https://doi.org/10.1103/PhysRevLett.17.1286.
[3] Zhao XP, Mofid SA, Gao T, Tan G, Jelle BP, Yin XB, et al. Durability-enhanced vanadium dioxide thermochromic film for smart windows. Mater Today Phys 2020;13:100205. https://doi.org/10.1016/j.mtphys.2020.100205.
[4] Chen S, Wang Z, Ren H, Chen Y, Yan W, Wang C, et al. Gate-controlled VO2 phase transition for high-performance smart windows. Sci Adv 2019;5:eaav6815. https://doi.org/10.1126/sciadv.aav6815.
[5] Ji H, Liu D, Cheng H, Zhang C. Inkjet printing of vanadium dioxide nanoparticles for smart windows. J Mater Chem C 2018;6:2424–9. https://doi.org/10.1039/C8TC00286J.
[6] Zheng J, Bao S, Jin P. TiO2(R)/VO2(M)/TiO2(A) multilayer film as smart window: combination of energy-saving, antifogging and self-cleaning functions. Nanomater Energy 2015;11:136–45. https://doi.org/10.1016/j.nanoen.2014.09.023.
[7] Zhou J, Gao Y, Zhang Z, Luo H, Cao C, Chen Z, et al. VO2 thermochromic smart window for energy savings and generation. Sci Rep 2013;3:1–5. https://doi.org/10.1038/srep03029.
[8] Sun G, Cao X, Zhou H, Bao S, Jin P. A novel multifunctional thermochromic structure with skin comfort design for smart window application. Sol Energy Mater Sol Cells 2017;159:553–9. https://doi.org/10.1016/j.solmat.2016.09.045.
[9] Kim H, Cheung K, Auyeung RCY, Wilson DE, Charipar KM, Piqué A, et al. VO2-based switchable radiator for spacecraft thermal control. Sci Rep 2019;9:1–8. https://doi.org/10.1038/s41598-019-47572-z.
[10] Sun K, Riedel CA, Urbani A, Simeoni M, Mengali S, Zalkovskij M, et al. VO2 thermochromic metamaterial-based smart optical solar reflector. ACS Photonics 2018;5:2280–6. https://doi.org/10.1021/acsphotonics.8b00119.
[11] Madiba IG, Émond N, Chaker M, Thema FT, Tadadjeu SI, Muller U, et al. Effects of gamma irradiations on reactive pulsed laser deposited vanadium dioxide thin films. Appl Surf Sci 2017;411:271–8. https://doi.org/10.1016/j.apsusc.2017.03.131.
[12] Hendaoui A, Émond N, Dorval S, Chaker M, Haddad E. VO2-based smart coatings with improved emittance-switching properties for an energy-efficient near room-temperature thermal control of spacecrafts. Sol Energy Mater Sol Cells 2013;117:494–8. https://doi.org/10.1016/j.solmat.2013.07.023.
[13] Benkahoul M, Chaker M, Margot J, Haddad E, Kruzelecky R, Wong B, et al. Thermochromic VO2 film deposited on Al with tunable thermal emissivity for space applications. Sol Energy Mater Sol Cells 2011;95:3504–8. https://doi.org/10.1016/j.solmat.2011.08.014.
[14] Amiche A, El Hassar SMK, Larabi A, Khan ZA, Khan Z, Aguilar FJ, et al. Innovative overheating solution for solar thermal collector using a reflective surface included in the air gap. Renew Energy 2019. https://doi.org/10.1016/j.renene.2019.11.023.
[15] Mercs D, Didelot A, Capon F, Pierson J-F, Hafner B, Pazidis A, et al. Innovative smart selective coating to avoid overheating in highly efficient thermal solar collectors. Energy Procedia 2016;91:84–93. https://doi.org/10.1016/j.egypro.2016.06.177.
[16] Paone A, Geiger M, Sanjines R, Schüler A. Thermal solar collector with VO2 absorber coating and V1-xWxO2 thermochromic glazing – temperature matching and triggering. Sol Energy 2014;110:151–9. https://doi.org/10.1016/j.solener.2014.08.033.
[17] Gurvitch M, Luryi S, Polyakov A, Shabalov A. Nonhysteretic behavior inside the hysteresis loop of VO2 and its possible application in infrared imaging. J Appl Phys 2009;106:104504. https://doi.org/10.1063/1.3243286.
[18] Son LN, Tachiki T, Uchida T. Characteristics of vanadium oxide thin films prepared by metal–organic decomposition for bolometer detectors. Jpn J Appl Phys 2011;50:025803. https://doi.org/10.1143/JJAP.50.025803.
[19] Xiao L, Ma H, Liu J, Zhao W, Jia Y, Zhao Q, et al. Fast adaptive thermal camouflage based on flexible VO2/graphene/CNT thin films. Nano Lett 2015;15:8365–70. https://doi.org/10.1021/acs.nanolett.5b04090.
[20] Kats MA, Blanchard R, Zhang S, Genevet P, Ko C, Ramanathan S, et al. Vanadium dioxide as a natural disordered metamaterial: perfect thermal emission and large broadband negative differential thermal emittance. Phys Rev X 2013;3:041004. https://doi.org/10.1103/PhysRevX.3.041004.
[21] Ji H, Liu D, Cheng H, Zhang C, Yang L. Vanadium dioxide nanopowders with tunable emissivity for adaptive infrared camouflage in both thermal atmospheric windows. Sol Energy Mater Sol Cells 2018;175:96–101. https://doi.org/10.1016/j.solmat.2017.10.013.
[22] Ji H, Liu D, Zhang C, Cheng H. VO2/ZnS core-shell nanoparticle for the adaptive infrared camouflage application with modified color and enhanced oxidation resistance. Sol Energy Mater Sol Cells 2018;176:1–8. https://doi.org/10.1016/j.solmat.2017.11.037.
[23] Ji C, Wu Z, Wu X, Wang J, Gou J, Huang Z, et al. Al-doped VO2 films as smart window coatings: reduced phase transition temperature and improved thermochromic performance. Sol Energy Mater Sol Cells 2018;176:174–80. https://doi.org/10.1016/j.solmat.2017.11.026.
[24] Sakai J, Zaghrioui M, Matsushima M, Funakubo H, Okimura K. Impact of thermal expansion of substrates on phase transition temperature of VO2 films. J Appl Phys 2014;116:123510. https://doi.org/10.1063/1.4896500.
[25] Radue E, Wang L, Kittiwatanakul S, Lu J, Wolf SA, Rossi E, et al. Substrate-induced microstructure effects on the dynamics of the photo-induced metal–insulator transition in VO2 thin films. J Optic 2015;17:025503. https://doi.org/10.1088/2040-8978/17/2/025503.
[26] Wang X, Cao Y, Zhang Y, Yan L, Li Y. Fabrication of VO2-based multilayer structure with variable emittance. Appl Surf Sci 2015;344:230–5. https://doi.org/10.1016/j.apsusc.2015.03.116.
[27] Paone A, Sanjines R, Jeanneret P, Whitlow HJ, Guibert E, Guibert G, et al. Influence of doping in thermochromic V1−xWxO2 and V1−xAlxO2 thin films: twice improved doping efficiency in V1−xWxO2. J Alloys Compd 2015;621:206–11. https://doi.org/10.1016/j.jallcom.2014.08.264.
[28] Krammer A, Magrez A, Vitale WA, Mocny P, Jeanneret P, Guibert E, et al. Elevated transition temperature in Ge doped VO2 thin films. J Appl Phys 2017;122:045304. https://doi.org/10.1063/1.4995965.
[29] Mlyuka NR, Niklasson GA, Granqvist CG. Mg doping of thermochromic VO2 films enhances the optical transmittance and decreases the metal-insulator transition temperature. Appl Phys Lett 2009;95:171909. https://doi.org/10.1063/1.3229949.
[30] Zhao Z, Liu Y, Wang D, Ling C, Chang Q, Li J, et al. Sn dopants improve the visible transmittance of VO2 films achieving excellent thermochromic performance for smart window. Sol Energy Mater Sol Cells 2020;209:110443. https://doi.org/10.1016/j.solmat.2020.110443.
[31] Li S-Y, Niklasson GA, Granqvist CG. Thermochromic undoped and Mg-doped VO2 thin films and nanoparticles: optical properties and performance limits for energy efficient windows. J Appl Phys 2014;115:053513. https://doi.org/10.1063/1.4862930.
[32] Dietrich MK, Kramm BG, Becker M, Meyer BK, Polity A, Klar PJ. Influence of doping with alkaline earth metals on the optical properties of thermochromic VO2. J Appl Phys 2015;117:185301. https://doi.org/10.1063/1.4919433.
[33] Xu G, Jin P, Tazawa M, Yoshimura K. Optimization of antireflection coating for

VO2-based energy efficient window. Sol Energy Mater Sol Cells 2004;83:29–37. https://doi.org/10.1016/j.solmat.2004.02.014.
[34] Jin P, Xu G, Tazawa M, Yoshimura K. Design, formation and characterization of a novel multifunctional window with VO2 and TiO2 coatings. Appl Phys A 2003;77:455–9. https://doi.org/10.1007/s00339-002-1460-2.
[35] Voti RL, Larciprete MC, Leahu G, Sibilia C, Bertolotti M. Optimization of thermochromic VO2 based structures with tunable thermal emissivity. J Appl Phys 2012;112:034305. https://doi.org/10.1063/1.4739489.
[36] Yu J-H, Nam S-H, Lee JW, Boo J-H. Enhanced visible transmittance of thermochromic VO2 thin films by SiO2 passivation layer and their optical characterization. Materials 2016;9:556. https://doi.org/10.3390/ma9070556.
[37] Kang L, Gao Y, Luo H, Wang J, Zhu B, Zhang Z, et al. Thermochromic properties and low emissivity of ZnO:Al/VO2 double-layered films with a lowered phase transition temperature. Sol Energy Mater Sol Cells 2011;95:3189–94. https://doi.org/10.1016/j.solmat.2011.06.047.
[38] Long S, Cao X, Li N, Xin Y, Sun G, Chang T, et al. Application-oriented VO2 thermochromic coatings with composite structures: optimized optical performance and robust fatigue properties. Sol Energy Mater Sol Cells 2019;189:138–48. https://doi.org/10.1016/j.solmat.2018.09.023.
[39] Kang Y-B. Critical evaluation and thermodynamic optimization of the VO–VO2.5 system. J Eur Ceram Soc 2012;32:3187–98. https://doi.org/10.1016/j.jeurceramsoc.2012.04.045.
[40] Xu X, Yin A, Du X, Wang J, Liu J, He X, et al. A novel sputtering oxidation coupling (SOC) method to fabricate VO2 thin film. Appl Surf Sci 2010;256:2750–3. https://doi.org/10.1016/j.apsusc.2009.11.022.
[41] García-Wong AC, Pilloud D, Bruyère S, Mathieu S, Migot S, Pierson JF, et al. Oxidation of sputter-deposited vanadium nitride as a new precursor to achieve thermochromic VO2 thin films. Sol Energy Mater Sol Cells 2020;210:110474. https://doi.org/10.1016/j.solmat.2020.110474.
[42] Rampelberg G, Schutter BD, Devulder W, Martens K, Radu I, Detavernier C. In situ X-ray diffraction study of the controlled oxidation and reduction in the V–O system for the synthesis of VO2 and V2O3 thin films. J Mater Chem C 2015;3:11357–65. https://doi.org/10.1039/C5TC02553B.
[43] Dou Y-K, Li J-B, Cao M-S, Su D-Z, Rehman F, Zhang J-S, et al. Oxidizing annealing effects on VO2 films with different microstructures. Appl Surf Sci 2015;345:232–7. https://doi.org/10.1016/j.apsusc.2015.03.044.
[44] Gomez-Heredia CL, Ramirez-Rincon JA, Ordonez-Miranda J, Ares O, Alvarado-Gil JJ, Champeaux C, et al. Thermal hysteresis measurement of the VO2 emissivity and its application in thermal rectification. Sci Rep 2018;8:1–11. https://doi.org/10.1038/s41598-018-26687-9.
[45] Zhang C, Yang Q, Koughia C, Ye F, Sanayei M, Wen S-J, et al. Characterization of vanadium oxide thin films with different stoichiometry using Raman spectroscopy. Thin Solid Films 2016;620:64–9. https://doi.org/10.1016/j.tsf.2016.07.082.
[46] Ureña-Begara F, Crunteanu A, Raskin J-P. Raman and XPS characterization of vanadium oxide thin films with temperature. Appl Surf Sci 2017;403:717–27. https://doi.org/10.1016/j.apsusc.2017.01.160.
[47] Parker JC. Raman scattering from VO2 single crystals: a study of the effects of surface oxidation. Phys Rev B 1990;42:3164–6. https://doi.org/10.1103/PhysRevB.42.3164.
[48] Schilbe P. Raman scattering in VO2. Phys B Condens Matter 2002;316–317:600–2. https://doi.org/10.1016/S0921-4526(02)00584-7.
[49] Baddour-Hadjean R, Pereira-Ramos JP, Navone C, Smirnov M. Raman microspectrometry study of electrochemical lithium intercalation into sputtered crystalline V2O5 thin films. Chem Mater 2008;20:1916–23. https://doi.org/10.1021/cm702979k.
[50] Yoon J, Park C, Park S, Mun BS, Ju H. Correlation between surface morphology and electrical properties of VO2 films grown by direct thermal oxidation method. Appl Surf Sci 2015;353:1082–6. https://doi.org/10.1016/j.apsusc.2015.07.036.
[51] Yu S, Wang S, Lu M, Zuo L. A metal-insulator transition study of VO2 thin films grown on sapphire substrates. J Appl Phys 2017;122:235102. https://doi.org/10.1063/1.4997437.
[52] Brassard D, Fourmaux S, Jean-Jacques M, Kieffer JC, El Khakani MA. Grain size effect on the semiconductor-metal phase transition characteristics of magnetron-sputtered VO2 thin films. Appl Phys Lett 2005;87:051910. https://doi.org/10.1063/1.2001139.
[53] Xu X, He X, Wang G, Yuan X, Liu X, Huang H, et al. The study of optimal oxidation time and different temperatures for high quality VO2 thin film based on the sputtering oxidation coupling method. Appl Surf Sci 2011;257:8824–7. https://doi.org/10.1016/j.apsusc.2011.04.068.

Alexis Carlos García Wong obtained a B.Sc in Physics (Summa Cum Laude) from the University of Havana, Cuba in 2012. He received a M.Sc in Physics from the Federal University of Pernambuco, Brazil in 2016. He is currently finishing a PhD in Materials Science at the Institut Jean Lamour, France. His research focuses on magnetron sputtering deposition, fabrication and characterization of thermochromic materials.

Denis Mangin obtained his B.S. in computer science from I.U.T. Charlemagne, Nancy in 1990 and M.S. from Conservatoire National des Arts et Métiers in 1995. From 1991 to 2013 he worked in Centre de Recherches Pétrographiques et Géochimiques, Vandoeuvre les Nancy, as an analyst on SIMS intruments (Caméca ims3f, ims1270 and ims1280). Since 2013 he is working as an engineer on a Caméca SIMS ims 7f in Institut Jean Lamour, Nancy.

Sylvie Migot was born in 1968. She obtained a Master in materials science in 1993. She worked during 21 years as technician at the University of Lorraine. She prepared samples and characterized them by X-Ray (Laue, Berg-Barret and Lang), optical microscopy, scanning electron microscopy (with EDS, EBSD) and transmission electron microscopy (with EDS). Now she is Engineer of the CNRS and she is responsible of two equipments in the Institut Jean Lamour: TEM Philips CM200 and SEM-FIB Helios Nanolab 600i. She is co-author of 55 papers.

Dr. Jean-François PIERSON is Professor of Materials Chemistry at the University of Lorraine (Ecole des Mines), Nancy, France. He obtained his PhD in 1997. He is currently the head of the department *Chemistry and Physics of Solids and Surfaces* at the Institut Jean Lamour (UMR CNRS 7198). His research is focused on the development of oxides and nitrides thin films for energy applications. He has published approx. 140 papers in peer-review journals and 6 patents.